Drainage conditions around monopiles in sand

Youhu Zhang, Shuzhao Li, Hans Petter Jostad

Shuzhao Li, PhD

Senior Geotechnical Engineer
CNOOC Research Institute Ltd.
CNOOC Plaza, No. 6, Taiyanggong South Street, Chaoyang District
Beijing, China, 100028
Telephone: +86 13521151037
Fax: +86 84525462
Email: lishzh17@cnooc.com.cn

Youhu Zhang (corresponding author), PhD

Technical Lead Offshore Geotechnics
Norwegian Geotechnical Institute
Sognsveien 72, 0855 OSLO
Telephone: +47 488 43 488
Fax: +47 22 23 04 48
Email: youhu.zhang@ngi.no

Hans Petter Jostad, PhD

Technical Director
Norwegian Geotechnical Institute
Sognsveien 72, 0855 OSLO
Telephone: +47 992 61 171
Fax: +47 22 23 04 48
Email: hans.petter.jostad@ngi.no

Revised manuscript submitted to *Applied Ocean Research* on November 28, 2018

No. of tables: 2

No. of figures: 7

Keywords: offshore wind turbines, monopile, drained, undrained, cyclic loading

1 Abstract

Large diameter monopiles are typical foundation solutions for offshore wind turbines. In design of the monopile foundations in sand, it is necessary to understand the drainage conditions of the foundation soil under the design loading conditions as the soil performance (strength and stiffness) is highly dependent on the drainage conditions. This paper presents a numerical investigation into this issue, with a purpose to develop a simple design criterion for assessing the soil drainage conditions around a monopile in sand. It is found that for typical monopile foundations in sand, the drainage condition during a single load cycle is generally expected to be undrained. However, the current state-of-practice uses *p-y* springs derived for drained soil responses for monopile design. The impact of this discrepancy on monopile foundation design was evaluated and found to be insignificant due to the relatively low level of loading as compared to the capacity of the soil.

2 Introduction

Large diameter monopile foundations are typical foundation solutions for offshore wind turbines. They are typically 5-10 m in diameter (D), and penetrated into the ground to provide support to the wind turbines. The typical penetration depth (L) over diameter (D) ratio (L/D) is around 5-6 or less.

In an optimum design of the monopile foundations in sand, it is necessary to understand the drainage conditions of the foundation soil under the design loading conditions. Soil performance (strength and stiffness) is highly dependent on the drainage conditions. For design of many onshore structures (except in earthquake design), sands are typically assumed to behave in a drained manner as the rate of loading is slow in comparison to the time needed to drain any excess pore pressure generated due to external loading. However, for offshore geotechnical designs, the environmental loading is typical cyclic in nature (e.g. wave loading). Sand can behave either drained, partially drained or fully undrained, depending on the rate of loading, drainage length and drainage properties of the sand. For design of gravity based structures (GBS), Madshus (1986) presented design charts for assessing the drainage conditions of GBS in sand for a range of boundary conditions based on assumption of isotropic linear elastic properties. However, to the authors' best knowledge, there is no design criterion that is readily available for evaluating the drainage conditions around an offshore monopile foundation.

Furthermore, the current state-of-practice in the industry is to design monopiles using the so-called "*p*-*y* curves" which represent the soil resistance along the pile in form of uncoupled non-linear load-displacement springs. The most commonly adopted *p*-*y* springs for design are according to the recommendation of API (2014)/DNV GL (2016). The API *p*-*y* springs for sand are developed from field pile testing, where the sand is loaded under drained conditions. The drained peak friction angle is used as a key model input parameter. Various laboratory 1g and Ng (i.e. centrifuge) monopile model testing has also been performed in either dry sand or the loading rate is too slow, resulting in essentially drained conditions (examples are, among others, Leblanc et al. (2009); Klinkvort and Hededal (2014); Li et al. (2015); Li et al. (2017); Nicolai et al. (2017)). The most recent comprehensive field pile testing program dedicated for developing soil-pile interaction models for monopile design, the PISA project (Byrne et al., 2017, Burd et al., 2017), also carried out the pile tests in sand under drained conditions. It appears that many of the monopiles in sand are designed today using *p*-*y* curves developed for drained soil response, which could differ from the actual conditions in-situ. The purpose of this work is also to examine the implications of this potential discrepancy.

This paper presents a numerical investigation into the above mentioned aspects in an effort to:

1) Develop a design criterion for assessing the soil drainage conditions around a monopile in sand;
2) Evaluate the potential implications of the current design practice of using *p*-*y* springs derived for drained soil responses.

3 Method

3.1 Finite element models

In this study, finite element analyses were performed using the commercial finite element package Plaxis 3D (Plaxis, 2013). Two finite element models were developed corresponding to the two main objectives set out above.

1) Disc model

To simplify the problem, a one-meter thick horizontal slice of the pile and the surrounding soil is considered, as illustrated in Figure 1a. Due to symmetry, only half of the pile cross-section is modelled. The top and bottom boundaries of the model are constrained from vertical displacement and water flow, whereas the horizontal boundaries are fixed in normal directions but allowed for free drainage (except for the vertical symmetry face, which is impermeable). This assumes that the drainage occurs within the horizontal plane. This is considered a reasonable assumption in the soil some distance below the mudline. Close to the mudline, preferential vertical drainage to the surface could occur which may speed up the drainage process. The impact of this assumption is later examined by full length pile analyses.

For the reference case, the diameter (D) of the monopile is 5 m. The horizontal boundary is chosen to be $12D$ from the centre of the monopile. The soil domain is discretised with coupled displacement-pore pressure elements. Increasingly refined mesh is used near the monopile to capture the high stress/pore pressure gradients. The monopile is modelled as a solid rigid continuum. Horizontal force is applied as a uniform pressure on the vertical symmetry surface of the monopile. In these analyses, soil-pile separation is not allowed.

Sensitivity analyses were performed to check the effect of the distance to the horizontal boundary, the mesh refinement and the time increment. The sensitivity analyses confirm that the currently adopted model produces satisfactory results.

2) Full pile length model

A full length pile model is also developed in order to evaluate the global pile response with regard to the drainage conditions. The model also serves the purpose of verifying the drainage criterion developed from the disc analyses. The monopile modelled herein has a diameter of 6 m and a uniform wall thickness of 0.06 m. The pile is penetrated 30 m (i.e. $5D$) into the ground, which consists of uniform, normally consolidated, Dogger Bank sand (Blaker and Andersen, 2015) with a relative density (D_r) of 80%. The horizontal load is applied 30 m above the mudline in order to generate representative overturning moment at mudline. The soil parameters are chosen based on calibration against soil element tests. Frictional pile-soil interface is assigned, which is allowed to gap if the normal contact stress reduces to zero. Further details on soil parameters and interface roughness factor are given in Section 3.3. It is noted that the pile diameter adopted in the full length model is 6 m, which is different from the disc analyses. However, since all the results will be presented in normalised format, it has no actual impact.

Due to symmetry, only half of the pile cross-section is modelled. The external sides of the model are free to drainage, except the vertical symmetry face of the model, which is impermeable. The model is as illustrated in Figure 1 (b).

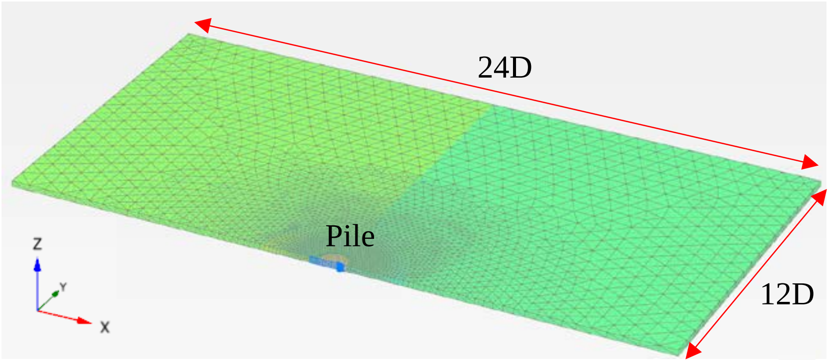

(a)

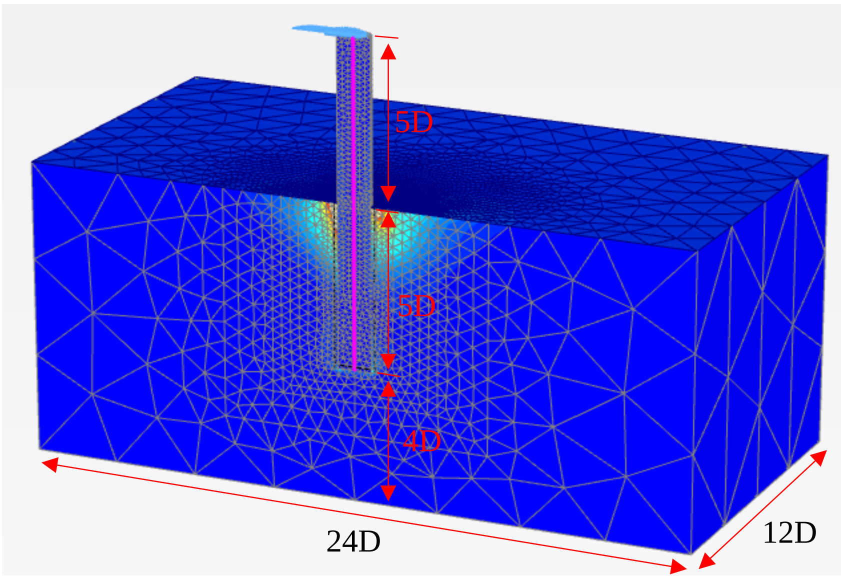

(b)

Figure 1. Illustration of the finite element models: a) disc model and b) full length pile model

3.2 Soil models

3.2.1 *Isotropic linear elastic model*

An isotropic linear elastic model is used in the disc analyses. The purpose of these analyses is to establish a preliminary framework for assessing the drainage conditions around the monopile, without the complication of the more realistic stress-dilatancy and stress level dependency of soil stiffness.

The elastic model is characterised by the Young's modulus E, Poisson's ratio υ, and permeability k. The constrained modulus M, defined as the stiffness in an oedometer condition, can be calculated as:

$$M = \frac{(1-\upsilon)E}{(1+\upsilon)(1-2\upsilon)} \tag{1}$$

The coefficient of consolidation c_v, which captures the combined effect of soil skeleton compressibility and pore water flow resistance (i.e. permeability), can be calculated as:

$$c_v = \frac{Mk}{\gamma_w} \tag{2}$$

where γ_w is the unit weight of the water, taken to be 10 kN/m^3.

3.2.2 *Hardening soil (HS) model*

The hardening soil (HS) model (Schanz et al., 1999) is used in the full length pile analyses. The model captures some important aspects of realistic soil behaviours, in particular non-linear shear hardening, shear induced dilatancy and stress level dependency of soil stiffness. The HS model is an effective stress based constitutive model for sand. The model adopts a Mohr-Coulomb (MC) failure criterion. Different from the conventional linear elastic, perfectly plastic MC model, it features a hyperbolic hardening law in shear, as illustrated in Figure 2.

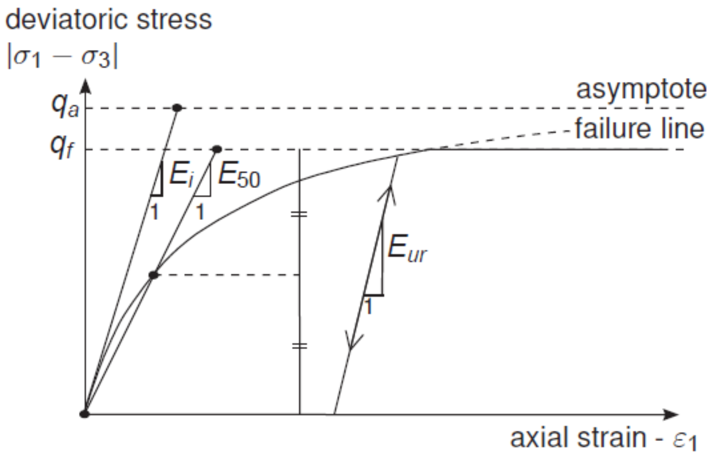

Figure 2. Hyperbolic stress-strain relation in a standard triaxial compression test (Plaxis, 2013)

The curvature of the hardening curve is controlled by the secant modulus at 50% mobilisation, E_{50}, which is assumed to be dependent on the minor principle stress by:

$$E_{50} = E_{50}^{ref}\left(\frac{\sigma_3^{'}}{p^{ref}}\right)^m \qquad (3)$$

where E_{50}^{ref} is a reference stiffness modulus corresponding to the reference stress p^{ref}, which is taken to be 100 kPa. σ_3' is the effective minor principle stress, and m determines the stress level dependency.

The unloading-reloading stiffness E_{ur} is also assumed to be stress level dependent. In this work, E_{ur} is taken to be $3E_{50}$, which is the recommended default value by Plaxis. Note that E_{ur} is considered as a true elastic material parameter. The elastic shear modulus G_{ur} can therefore be calculated from E_{ur} by:

$$G_{ur} = \frac{E_{ur}}{2(1+\upsilon)} \qquad (4)$$

where υ is the Poisson's ratio and taken to be 0.2.

The HS soil model also features a compression cap in order to capture the plastic volumetric deformation during virgin compression. The constrained modulus during virgin compression, denoted as E_{oed} in the hardening soil model, is also taken to be stress level dependent by:

$$E_{oed} = E_{oed}^{ref}\left(\frac{\sigma_1^{'}}{p^{ref}}\right)^m \tag{5}$$

where σ_1' is the effective major principle stress. In this work, the sand was simulated as normally consolidated.

3.3 Determination of HS soil model parameters

Blaker and Andersen (2015) presented a set of laboratory tests on very dense fine to medium Dogger Bank sand under drained and undrained conditions. The test samples are clean sand with fines content less than 1% and d_{10} and d_{60} equal to 0.087 mm and 0.174 mm respectively. The grain size distribution of Dogger Bank sand is representative for typical sands encountered in the North Sea. Triaxial compression tests were conducted on anisotropically consolidated samples prepared by moist tamping to a relative density D_r of 80%. Two vertical consolidation stresses (σ'_{vc} = 40kPa and 200kPa) were tested, while a K_0 value of 0.45 was used in all tests. The parameters of the HS model were calibrated by back calculation of those triaxial tests and the comparisons between model simulations and lab test results are illustrated in Figure 3 and Figure 4 for drained and undrained tests respectively. It can be seen that the HS model is able to reproduce the lab results very well. It should be noted that in the drained compression test, post peak softening response is observed. However, this cannot be captured by the HS soil model. As will be discussed in Section 5, monopile is designed with stringent displacement criterion. The strain level in the soil is small therefore the strain softening effect at larger strains is considered insignificant, particularly as the drainage level approaches undrained conditions. The value of the reference constrained modulus E_{oed}^{ref} was chosen to produce a good fit to the undrained tests. It is found to be approximately twice the value that is suggested by the oedometer test. Since the results will be presented in normalised form (Section 4.1), the exact value of E_{oed}^{ref} does not influence the normalised results. Based on the calibration exercise, the model parameters as listed in Table 1 were chosen for the full length pile analyses.

Table 1. Summary of HS model parameters for full length pile analysis

Parameter	Value
E_{50}^{ref}, MPa	160
E_{ur}^{ref}, MPa	480
E_{oed}^{ref}, MPa	110
v, -	0.2
φ', °	44
ψ, °	20
p^{ref}, kPa	100
m, -	0.5
R_f, -	0.9
K_{0nc}, -	0.305
γ', kN/m^3	10
e_{ini}, -	0.651
e_{max}, -	0.865
e_{min}, -	0.597

The initial void ratio (e_{ini}), max void ratio (e_{max}) and minimum void ratio (e_{min}) were specified so that dilatancy will stop once the void ratio reaches the maximum value. In addition, the sand is assumed to be isotropic in terms of permeability. A constant value of k= 2.4E-5 m/s was used in the analyses. The change of the permeability due to void ratio change is not taken into account as it is considered to be secondary effect.

Frictional pile-soil interface is assigned, which is allowed to gap if the normal contact stress reduces to zero. The interface friction angle is chosen to be 30°, which represent a roughness factor of 0.6.

The cavitation pressure is dependent on the water depth and soil depth in question. In the current analyses, no cavitation limit is assigned. In an actual design scenario, this needs to be considered to ensure mobilised negative pore pressure does not exceed the actual cavitation limit.

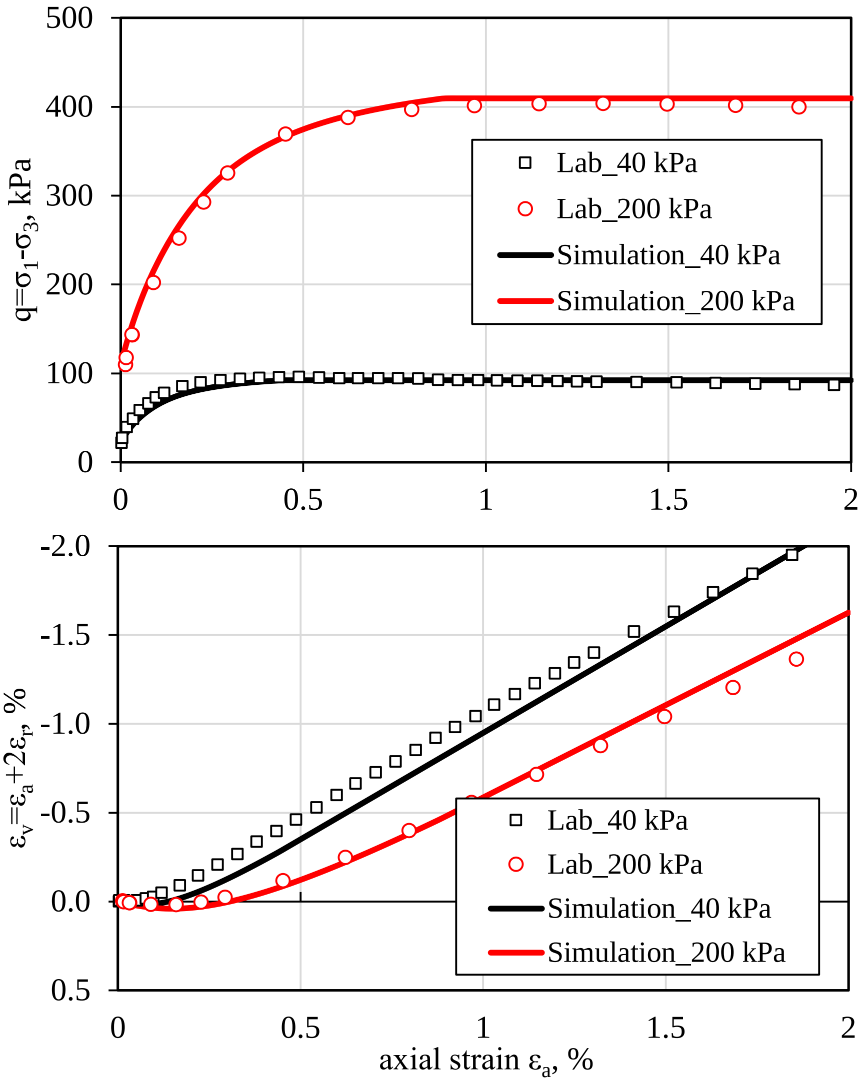

Figure 3. Comparison of HS model simulations with lab results of two drained triaxial compression tests anisotropically consolidated under 40 and 200 kPa vertical stress (K_0=0.45)

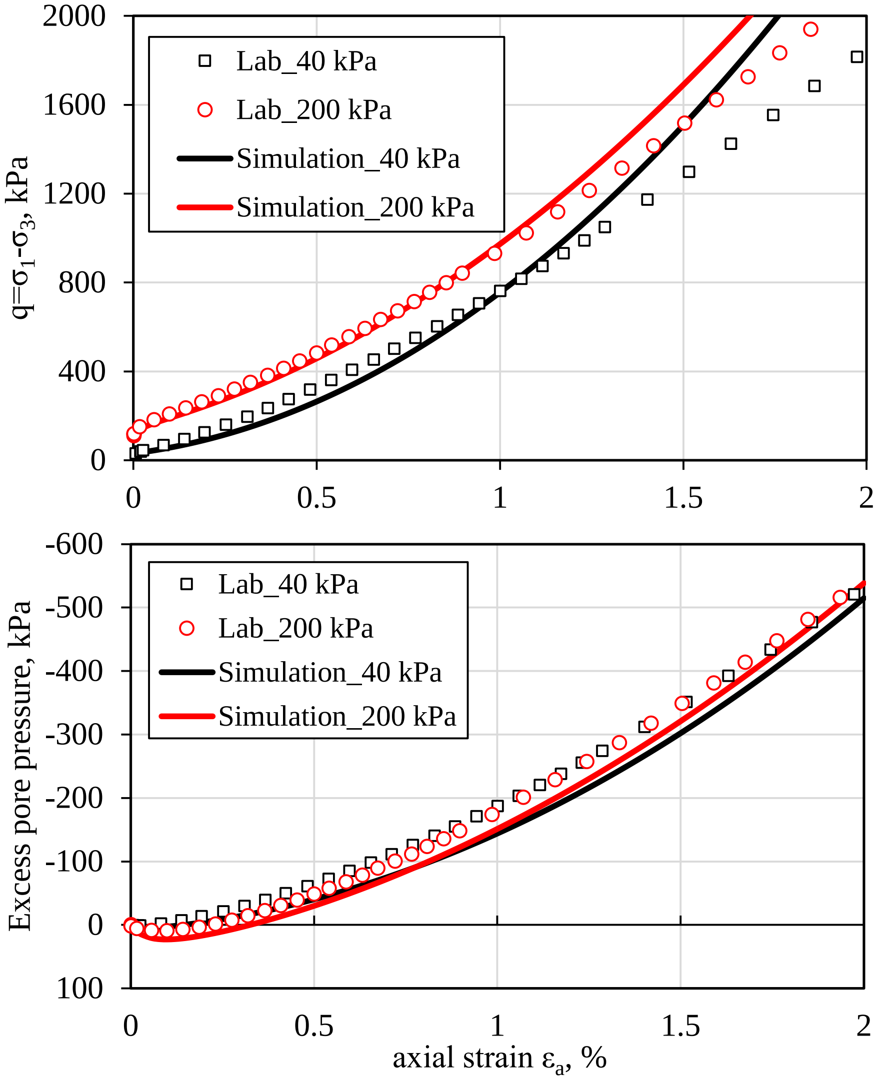

Figure 4. Comparison of HS model simulations with lab results of two undrained triaxial compression tests anisotropically consolidated under 40 and 200 kPa vertical stress (K_0=0.45)

Figure 5 compares the stress-strain paths obtained from the laboratory triaxial compression tests performed under drained and undrained conditions. It can be seen that the stress-strain responses are very similar before soil dilatancy governs the behaviour, which deviates the undrained responses from the drained responses.

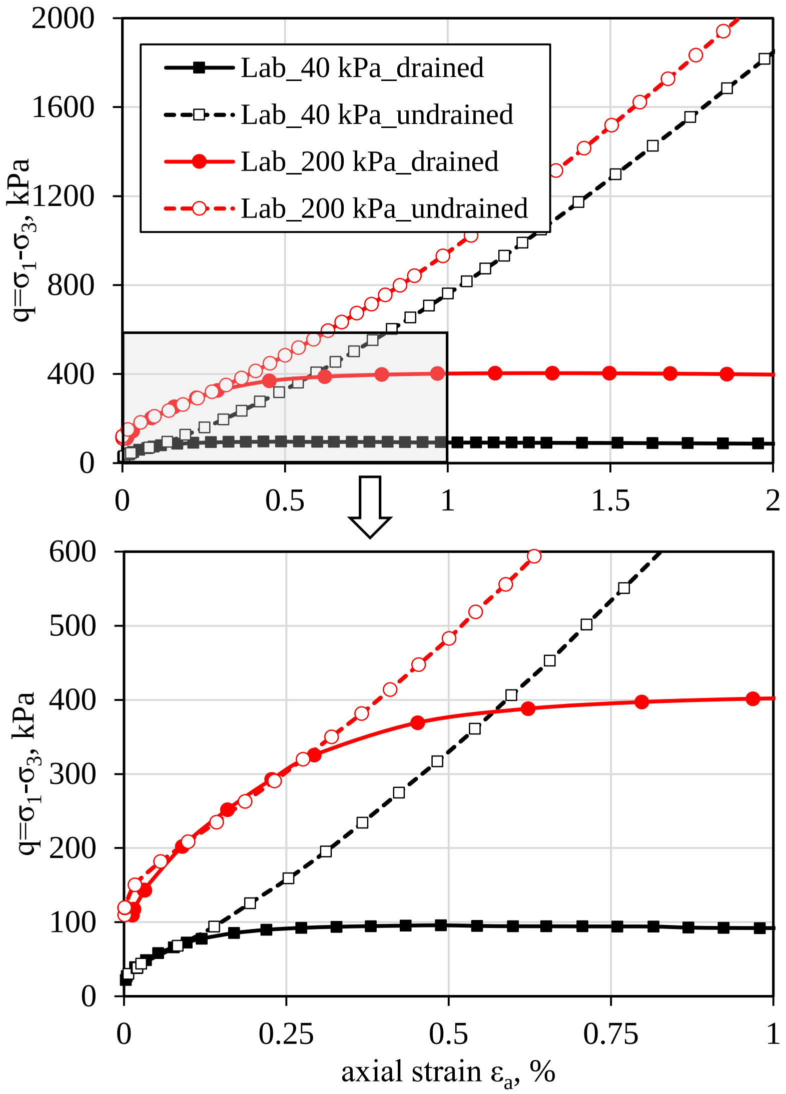

Figure 5. Comparison between drained and undrained triaxial compression test results

3.4 Analyses

3.4.1 *Pile disc analyses with linearly elastic soil model*

A cyclic sinusoidal force is applied to pile section. The pore pressure is generated and dissipated simultaneously. Parametric analyses were performed to cover a wide range of normalised loading periods (i.e. T_p as will be defined in Section 4) so that soil responses from fully drained to fully undrained were examined. The same cyclic loading is applied in all analyses. However, it should be noted that in these elastic analyses, the pore pressure response is proportional to the loading level. When it is normalized by the applied load, a uniform set of response is obtained.

3.4.2 *Full length pile analyses with HS soil model*

As the HS model is not suited for cyclic loading, a monotonic pile head lateral loading is applied, simulating the first quarter of a load cycle. A range of normalised loading periods (i.e. T_p as will be defined in Section 4) were examined, matching those in the disc analyses. The global pile response is then examined.

4 Results from disc analyses

4.1 Normalisation of results

In order to present the numerical results in a generalised framework, the results are normalised in the following format:

Normalised excess pore pressure P

$$P = u / p \tag{6}$$

where u is the calculated excess pore pressure at the point of interest; p is the average bearing pressure exerted on the pile slice, which is calculated as the applied force divided by the laterally projected area of the pile slice.

Normalised loading period T_p

$$T_p = t_p c_v \big/ D^2 \tag{7}$$

where t_p is the cyclic loading period; c_v is the coefficient of consolidation.

A comprehensive parametric analyses were performed to confirm the appropriateness of the chosen normalisation, including different pile diameter D, soil permeability k, and Poisson's ratio v.

4.2 Results from disc analyses

Figure 6 presents the stabilised pore pressure response at the peak of cyclic loading (i.e. when the applied lateral load is at the maximum) from different analyses. Each curve represents one analysis, which has a specific normalised loading period T_p. The results cover the range from fully undrained conditions to almost fully drained conditions. Additional analyses with smaller T_p value than 0.5 reveal almost identical pore pressure distribution as analysis with T_p=0.05, which implies that for a T_p equal or less than 0.5, an essentially undrained soil response can be expected. However, for clarity, those additional analyses are not presented in Figure 6. Whereas if T_p is greater than 50, the pore response is negligible, and for all practical purposes the soil can be essentially treated as drained. This set of curves can be used as a preliminary criterion to evaluate the drainage conditions around a monopile under cyclic loading.

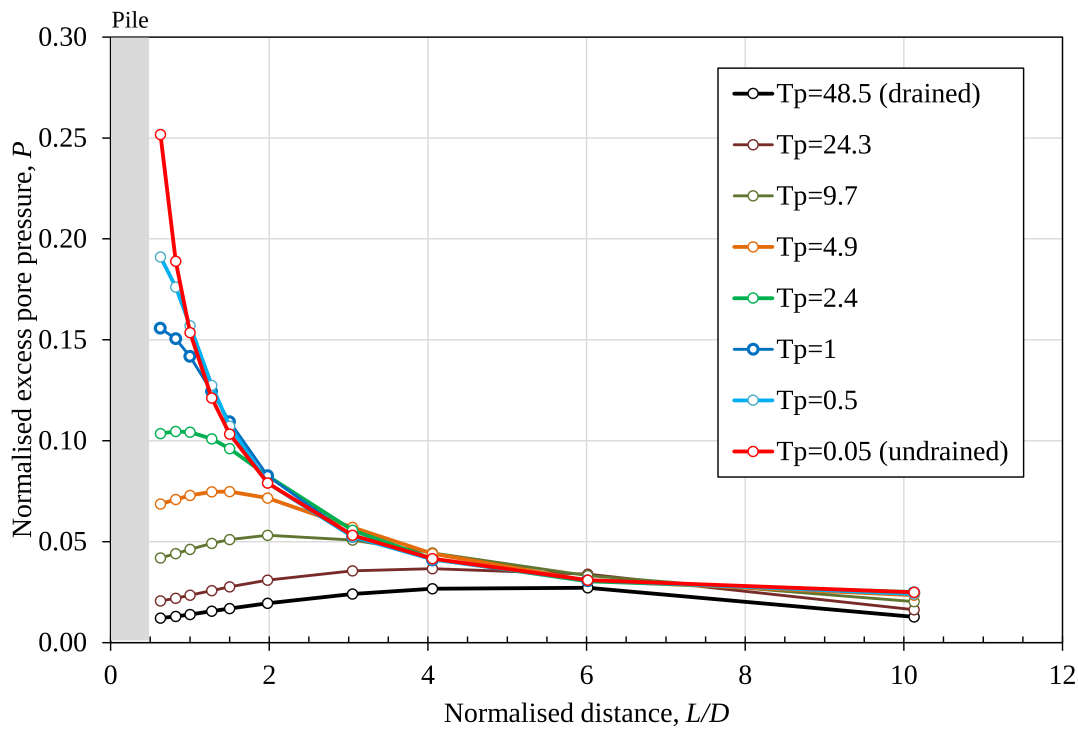

Figure 6. Normalised pore pressure response at peak cyclic load versus normalised distance and normalised loading period

In Table 2, the normalised time factor T_p for a monopile with a diameter of 5 m is evaluated for a range of permeability, cyclic loading periods (considering the different forcing frequencies on monopiles, i.e. rotational frequency 1P, blade passing frequency 3P and wave frequency) and constrained modulus (which is a function of effective mean stress level, i.e. soil depth; relative density; load path, i.e. virgin loading/unloading/reloading). To put the results in context, the 1P period range for a Vestas V164-8.0 MW offshore wind turbine is 5 to 12.5 s (Arany et al., 2016). The 3P period is 1/3 of the 1P period, i.e. from 1.7 to 4.2 s. The typical wave period is around 10 s. Compared with the criterion established in Figure 6, it can be seen that essentially undrained response will be expected within a single cycle in typical North Sea sands. Even for a relatively high permeability k=1E-3 m/s, partially drained response will still be expected. It is also worth noting that that the trend in the industry is to use larger diameter monopiles as turbine capacity increases, and 8-10 m diameter piles have become the norm of today. This will further reduce the level of drainage during a load cycle.

Table 2. Normalised T_p factor for a 5m diameter monopile for different constrained modulus, permeability and cyclic loading period

M, MPa	t_p, s	k, m/s		
		1.0E-03	1.0E-04	1.0E-05
20	2.5	T_p=0.20	0.020	0.002
	5	0.40	0.040	0.004
	10	0.80	0.080	0.008
50	2.5	0.50	0.050	0.002
	5	1.00	0.100	0.004
	10	2.00	0.200	0.008
100	2.5	1.00	0.100	0.010
	5	2.00	0.200	0.020
	10	4.00	0.400	0.040

4.3 Results from full length pile analyses with HS model analyses

This section presents results from the full length pile analyses using the HS soil model. Due to inability to simulate cyclic loading with the adopted soil model, monotonic loading is applied to the pile head to simulate the pile response during the first quarter of a load cycle. A range of normalised loading rates were considered. The purpose of these analyses were two-fold: i) to verify the drainage criterion established from the simple disc analyses using the elastic soil model; ii) to assess the implications of drainage condition with regard to monopile design.

Along the length of a monopile, the constrained modulus M, equivalent to E_{oed} in HS model, increases with depth as stress level increases. To characterise the loading rate, the T_p value is calculated using the constrained modulus at in-situ stress level at mid depth of the pile, i.e. 15 m below the mudline.

Figure 7(a) presents the load-displacement curves at mudline level from seven coupled analyses and two analyses where soil is formulated drained and undrained respectively. In the fully drained analysis, the total stress change is taken as effective stress change, whereas in the fully undrained analysis, approximately zero volumetric strain is enforced at every integration point of the soil domain by including a numerically high bulk modulus for the pore water. It can be seen that at a normalized loading period of T_p = 90, the load-displacement curve compares closely to the results of the fully drained analysis. Whereas at a normalized loading period of T_p = 0.09, the load-displacement curve is almost identical to result of the undrained analysis. As T_p value increases, the global pile response gradually transits from the undrained to the drained conditions. The results from full length pile analyses suggest that the drainage criterion established from the simple disc analyses, does indeed provide a reasonable indication of the drainage conditions of the soil around the monopile.

The results presented in Figure 7 also illustrates that stiffer response is obtained under undrained conditions than under drained conditions. This is as expected for the dense sand considered herein, which dilates under shear deformation. The dilation in turn enhance soil strength and stiffness if drainage does not have sufficient time to occur under partially drained to undrained conditions due to generation of negative pore pressure (i.e. effective stress increases).

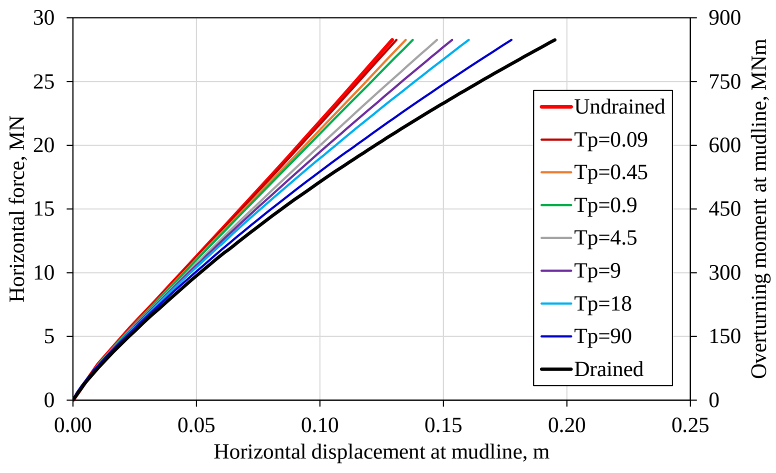

(a) Load-deflection at mudline

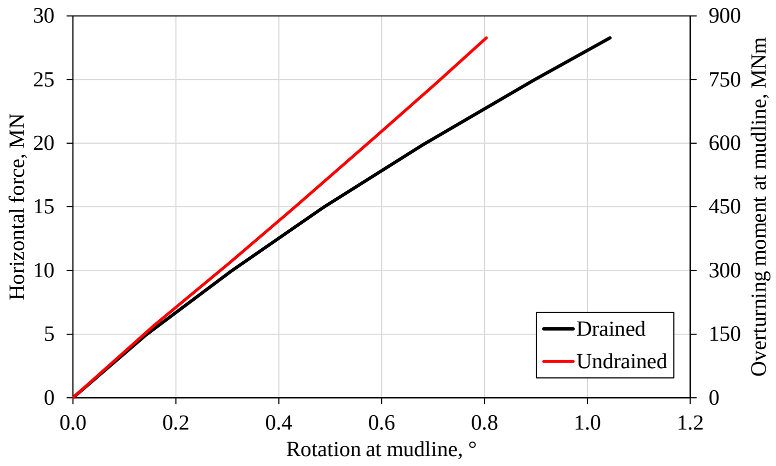

(b) Moment-rotation at mudline

Figure 7. Load-displacement (moment-rotation) responses at mudline level at various normalised loading rate T_p

5 Discussions and implication for monopile design

In this study, a criterion is developed for assessing the soil drainage conditions around a monopile foundation in sand within a single load cycle. Based on this criterion, it is found that undrained soil response is generally expected for monopiles of today's size in typical sandy soils within a single load cycle. However, the state-of-practice for monopile design uses soil reaction models developed for drained loading conditions. The implication of this discrepancy for the monopile design is discussed below.

The International Electrotechnical Commission code (IEC, 2009) describes many load cases to be considered for offshore wind turbine foundation design with different combinations of wind and sea states. Two example scenarios are discussed below. When the wind turbine is under normal power production, a significant portion of the environmental load acting on the monopile foundation comes from the wind thrust exerted on the turbine blades. The average wind load, representing the force due to mean wind speed, can be reasonably expected to be reacted in a drained manner in sandy soils. The cyclic load component caused by structural vibrations as a result of wave, 1P and 3P excitations, however, is expected to be reacted in an undrained manner by the soil during a single load cycle, based on the criterion developed above. When the turbine is parked, for example, under extreme environmental conditions, the turbine blades are pitched out of the wind. The wind load reduces and a larger proportion of the total environmental load on the monopile may come from the wave loading on the tower which is expected to be reacted undrained during a single load cycle. It can be seen that the loading condition on the monopile foundation is rather complex and depends on the load case considered. A certain portion of the environmental loading is reacted by the soil in a drained manner while the remaining reacted by the soil in an undrained condition.

However, it should also be noted that monopile foundations are designed with stringent serviceability requirement. For example, DNV GL (2016) suggest to limit the mudline rotation due to environmental loading to 0.25°, in addition to an installation tolerance of 0.25°. Referring to Figure 7(b), it can be seen the pile moment-rotation response at mudline is almost identical between drained and undrained conditions when the mudline rotation is less than 0.25°. The reason is best explained by Figure 5, which illustrates that before the dilatancy effects govern the soil response, the stress strain paths experienced by the soil are almost identical, regardless of the drainage conditions. This is embodied by the global behaviour shown in Figure 7. Based on this, despite that the drainage conditions have a significant impact on the pile response at large load, the influence on pile stiffness is negligible at load levels relevant for monopile design, which are low compared to the ultimate capacity of the pile. The implication of the discrepancy between the design assumption (drained condition) and actual condition (undrained condition during a single load cycle) is therefore insignificant.

It should be borne in mind that the current analyse have not taken into account of the cyclic effects and potential accumulation of pore pressure due to repeated load cycles. However, it is also known that under low mobilisation levels, the pore pressure generated and accumulated due to cyclic loading is small. Nevertheless, the effect of cyclic loading, and how it impacts the above conclusion should be further investigated.

6 Acknowledgements

The authors wish to gratefully acknowledge the financial support received through a NGI internal strategic research project SP9: Behaviour of Sand under Partial Drainage and Offshore Foundation Design, which is funded by the Norwegian Research Council through an annual base funding to NGI. The first author wish to acknowledge the mobility funding from the China Natural Science Foundation (funding no. 2016M600177) which supported her visit to NGI in

2017. The authors also wish to thank colleagues at NGI for valuable discussions, in particular, Ms Ana Page, Dr Hendrik Sturm and Dr Rasmus Tofte Klinkvort.

7 References

API RP 2GEO (2014). Recommended Practice for Geotechnical and Foundation Design Considerations, 1st Edition Addendum 1.

Arany, L., Bhattacharya, S., Macdonald, J.H.G. and Hogan, S.J. (2016). Closed form solution of Eigen frequency of monopile supported offshore wind turbines in deeper waters incorporating stiffness of substructure and SSI. Soil Dynamics and Earthquake Engineering, 83 (2016), page 18-32.

Blaker, Ø. and Andersen K.H. (2015). Shear strength of dense to very dense Dogger Bank sand. Frontiers of Offshore Geotechnics III-Meyer (Ed.). 2015 Taylor Francis Group, London, page 1167-1172.

Burd, H.J., Byrne, B.W., McAdam, R.A., Houlsby, G.T., Martin, C.M., Beuckelaers, W.J.A.P., Zdravkovic, L., Taborda, D.M.G., Potts, D.M., Jardine, R.J., Gavin, K., Doherty, P., Igoe, D., Skov Gretlund, J., Pacheco Andra, M., Muir Wood, A.(2017). Design aspects for monopile foundations. *Proceedings of TC 209 workshop, 19th ICSMGE – Seoul.*

Byrne, B.W., McAdam, R.A., Burd, H.J., Houlsby, G.T., Martin, C.M., Beuckelaers, W.J.A.P., Zdravkovic, L., Taborda, D.M.G., Potts, D.M., Jardine, R.J., Ushev, E., Liu, T., Abadias, D., Gavin, K., Igoe, D., Doherty, P., Skov Gretlund, J., Pacheco Andra, M., Muir Wood, A., Schroeder, F.C. Turner, S. and Plummer M.A.L. (2017). PISA: new design methods for offshore wind turbine monopiles. OSIG 2017, *Proceedings of the 8th International Conference Offshore Site Investigation and Geotechnics*, *Smater Solutions for Future Offshore Developments*, 142-161.

DNVGL-ST-0126 (2016). Support structures for wind turbines, edition April 2016.

IEC 61400-3: Wind turbines - Part 3: Design requirements for offshore wind turbines (2009). International Electrotechnical Commission (IEC).

Klinkvort, R.T. and Hededal, O. (2014). Effect of load eccentricity and stress level on monopile support for offshore wind turbines. Canadian Geotechnical Journal, Vol 51, 966-974.

Leblanc, C., Houlsby, G.T. and Byrne, B.W. (2009). Response of stiff piles in sand to long-term cyclic lateral loading. Geotechnique, Vol 60, Issue 2, 79-90.

Li, W., Igoe, D. and Gavin, K. (2015). Field tests to investigate the cyclic response of monopiles in sand. *Geotechnical Engineering*, Vol 168. Issue GE5, 407-421.

Li, W., Zhu, B. and Yang, M. (2017). Static response of monopile to lateral load in overconsolidated dense sand. Journal of Geotechnical and Geoenvironmental Engineering, ASCE, 04017026-1.

Madshus C (1986). Foundation engineering criteria for gravity platforms: cyclic pore pressure in sand subjected to harmonic and stochastic loading – analytical solutions. NGI report: 40013-8.

Nicolai, G., Ibsen, L.B., O'Loughlin, C.D. and White, D.J. (2017). Quantifying the increase in lateral capacity of monopiles in sand due to cyclic loading. *Geotechnique Papers* 7, 1-8.

Plaxis (2013). Plaxis 3D reference manual 2013.

Schanz T, Vermeer, PA and Bonnier, PG (1999). The hardening soil model: formulation and verification. Beyond 2000 in Computational Geotechnics – 10 Year of Plaxis. Balkema, Rotterdam, ISBN 90 5809 040 X.